

## ON THE SCATTERING OF ELECTROMAGNETIC WAVES BY A DIELECTRIC CYLINDER\*

BY

WILLIAM STREIFER\*\* AND RALPH D. KODIS†

*Brown University, Providence, R.I.*

**Abstract.** The scattering of  $E$ -polarized cylindrical electromagnetic waves by an infinitely long dielectric cylinder is investigated. For small incident wavelength the slowly converging series solution is converted to a sum of integrals. An expansion is performed so that the integrals may be divided into two classes depending on the relative locations of source and observation points. Those in the first class have points of stationary phase and an asymptotic evaluation gives contributions which are identified as those of geometric optics. The remaining integrals are evaluated as residue sums. A plot of normalized back-scattering cross section vs. normalized radius for  $n = .4$  is given.

**Introduction.** The scattering of electromagnetic waves by an infinite dielectric cylinder of large radius has been treated by Beckmann and Franz [1], [2] among others. They employ the Watson transformation to convert the slowly convergent series solution into a sum of integrals, some of which are evaluated by the method of stationary phase and yield geometric optics terms. The remainder are transformed to residue sums and interpreted as diffraction effects. The pole locations they use in evaluating these residues are only qualitatively determined.

In the following the authors employ the Poisson sum formula as suggested by Wu [3] to obtain integrals similar to those found by Beckmann and Franz. However, the present work is an extension of theirs in three respects: (1), more precise pole locations are used in the residue computation; (2), the refractive index of the cylinder is taken to be less than one; and (3), numerical results are included.

**Formulation.** If an electromagnetic wave emanates from an infinite line source with its electric vector parallel to the axis of an infinite dielectric cylinder, the governing equation in the coordinate system illustrated in Fig. 1 is

$$[\nabla_{r,\theta}^2 + k^2(r)]G(\mathbf{r}, \mathbf{r}') = -\delta(\mathbf{r} - \mathbf{r}'), \quad (1)$$

where  $k(r)$  equals  $k_1$  for  $r < a$  and  $k_2$  for  $r > a$ ;  $k_1$  and  $k_2$  are real. The function  $G(\mathbf{r}, \mathbf{r}')$ , together with its derivative  $\partial_r G(\mathbf{r}, \mathbf{r}')$ , is continuous at the cylinder surface  $r = |\mathbf{r}| = a$  and satisfies the radiation condition

$$\lim_{r \rightarrow \infty} [r^{1/2}(\partial_r - ik_2)G] = 0.$$

The solution of (1) in  $r \geq a$ , found by separation of variables, is

$$G(\mathbf{r}, \mathbf{r}') = (i/8) \sum_{n=-\infty}^{+\infty} \{H_n^{(1)}(k_2 r') H_n^{(2)}(k_2 r) + H_n^{(1)}(k_2 r') H_n^{(1)}(k_2 r) [H_n^{(2)}(x)/H_n^{(1)}(x)] R(n)\} \exp(in\theta), \quad (2a)$$

---

\*Received September 23, 1963; revised manuscript received December 20, 1963.

\*\*Now at University of Rochester.

†Now at Lincoln Laboratories, MIT.

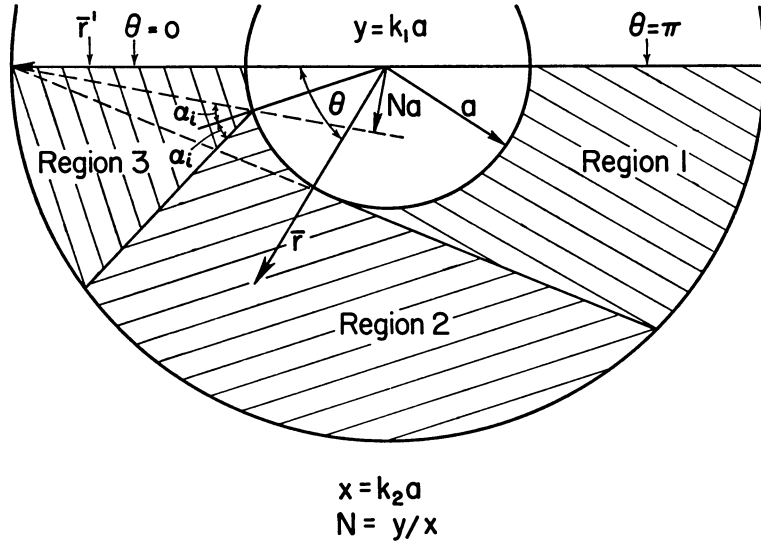


FIG. 1. Regions for observation points.

where

$$R(n) = -C_2(n)/C_1(n), \tag{2b}$$

$$C_{1,2}(n) = xH_n^{(1),(2)'}(x)/H_n^{(1),(2)}(x) - yJ_n'(y)/J_n(y),$$

(the superscript (1) refers to  $C_1$ ) and

$$x = k_2 a, \quad y = k_1 a.$$

The line source may be at either the primed or unprimed point, provided  $r' > r$ .

For large cylinders, i.e.  $x, y \gg 1$ , the series (2a) converges very slowly, and it is convenient to employ the Poisson sum formula [3] to obtain

$$G(\mathbf{r}, \mathbf{r}') = (i/8) \sum_{m=-\infty}^{+\infty} \int_{-\infty}^{+\infty} \{ H_\nu^{(1)}(k_2 r') H_\nu^{(2)}(k_2 r) + H_\nu^{(1)}(k_2 r') H_\nu^{(1)}(k_2 r) [H_\nu^{(2)}(x)/H_\nu^{(1)}(x)] R(\nu) \} \exp [i\nu(\theta + 2\pi m)] d\nu. \tag{3}$$

When Debye's asymptotic forms for the Hankel and Bessel functions [4] are substituted in (3) it is evident that for  $0 \leq \theta \leq \pi$  every integral with  $m \geq 0$  has many stationary phase points. These contributions may be separated by expanding  $R(\nu)$  (see Appendix A):

$$R(\nu) = R_1(\nu) + (1 + R_1)(1 + R_2) \sum_{p=+1}^{+\infty} R_2^{p-1} [H_\nu^{(1)}(y)/H_\nu^{(2)}(y)]^p, \tag{4}$$

where

$$R_{1,2}(\nu) = -[L(\nu)]^{-1} \{ xH_\nu^{(2),(1)'}(x)/H_\nu^{(2),(1)}(x) - yH_\nu^{(2),(1)'}(y)/H_\nu^{(2),(1)}(y) \},$$

(the superscript (2) refers to  $R_1$ ) and

$$L(\nu) = xH_\nu^{(1)'}(x)/H_\nu^{(1)}(x) - yH_\nu^{(2)'}(y)/H_\nu^{(2)}(y).$$

Substituting (4) in (3), interchanging summation and integration, and carrying out various algebraic manipulations, we obtain:

$$(8/i)G(\mathbf{r}, \mathbf{r}') = \sum_{m=-\infty}^{-1} \int_{-\infty}^{+\infty} \{H_{\nu}^{(1)}(k_2 r') H_{\nu}^{(2)}(k_2 r) + H_{\nu}^{(1)}(k_2 r') H_{\nu}^{(1)}(k_2 r) [H_{\nu}^{(2)}(x)/H_{\nu}^{(1)}(x)] R(\nu)\} \exp [i\nu(\theta + 2\pi m)] d\nu \quad (5a)$$

$$+ \sum_{m=+1}^{+\infty} \int_{-\infty}^{+\infty} \{H_{\nu}^{(1)}(k_2 r') H_{\nu}^{(2)}(k_2 r) + H_{\nu}^{(1)}(k_2 r') H_{\nu}^{(1)}(k_2 r) [H_{\nu}^{(2)}(x)/H_{\nu}^{(1)}(x)] R(-\nu)\} \exp [i\nu(\theta + 2\pi m)] d\nu \quad (5b)$$

$$+ \sum_{\nu=+1}^{+\infty} \sum_{m=+1}^{\nu-1} \int_{-\infty}^{+\infty} \{H_{\nu}^{(1)}(k_2 r') H_{\nu}^{(1)}(k_2 r) [H_{\nu}^{(2)}(x)/H_{\nu}^{(1)}(x)] \cdot (1 + R_1)(1 + R_2) R_2^{\nu-1} [H_{\nu}^{(1)}(y)/H_{\nu}^{(2)}(y)]^{\nu} \exp [i\nu(\theta + 2\pi m)] d\nu \quad (5c)$$

$$+ \int_{-\infty}^{+\infty} \{H_{\nu}^{(1)}(k_2 r') H_{\nu}^{(2)}(k_2 r) + H_{\nu}^{(1)}(k_2 r') H_{\nu}^{(1)}(k_2 r) [H_{\nu}^{(2)}(x)/H_{\nu}^{(1)}(x)] R_1(\nu)\} \exp (i\nu\theta) d\nu \quad (5d)$$

$$+ \sum_{\nu=+1}^{+\infty} \int_{-\infty}^{+\infty} \{H_{\nu}^{(1)}(k_2 r') H_{\nu}^{(1)}(k_2 r) [H_{\nu}^{(2)}(x)/H_{\nu}^{(1)}(x)] \cdot (1 + R_1)(1 + R_2) R_2^{\nu-1} [H_{\nu}^{(1)}(y)/H_{\nu}^{(2)}(y)]^{\nu} \exp (i\nu\theta) d\nu \quad (5e)$$

$$- (8/\pi^2) \int_{-\infty}^{+\infty} \frac{H_{\nu}^{(1)}(k_2 r') H_{\nu}^{(1)}(k_2 r) \exp (i\nu\theta) d\nu}{[H_{\nu}^{(1)}(x)]^2 H_{\nu}^{(2)}(y) J_{-\nu}(y) L(\nu) C_1(-\nu)}. \quad (5f)$$

Each of the integrals (5a)–(5f) which has a stationary phase point yields a characteristic ray of geometric optics. Some of these rays can reach only a restricted region which depends upon the relative position of source and observation points. With the index of refraction  $N = y/x < 1$  and the observation point at  $r < r'$ , three regions can be distinguished (see Fig. 1).

**Region 1.** In this, the "shadow" region, it is convenient to rewrite  $G(\mathbf{r}, \mathbf{r}')$  in the form:

$$G(\mathbf{r}, \mathbf{r}') = (i/8) \sum_{m=-\infty}^{-1} \int_{-\infty}^{+\infty} \{H_{\nu}^{(1)}(k_2 r') H_{\nu}^{(2)}(k_2 r) + H_{\nu}^{(1)}(k_2 r') H_{\nu}^{(1)}(k_2 r) [H_{\nu}^{(2)}(x)/H_{\nu}^{(1)}(x)] R(\nu)\} \exp [i\nu(\theta + 2\pi m)] d\nu \quad (6a)$$

$$+ (i/8) \sum_{m=0}^{+\infty} \int_{-\infty}^{+\infty} \{H_{\nu}^{(1)}(k_2 r') H_{\nu}^{(2)}(k_2 r) + H_{\nu}^{(1)}(k_2 r') H_{\nu}^{(1)}(k_2 r) [H_{\nu}^{(2)}(x)/H_{\nu}^{(1)}(x)] R(-\nu)\} \exp [i\nu(\theta + 2\pi m)] d\nu \quad (6b)$$

$$+ (i/8) \sum_{\nu=+1}^{+\infty} \sum_{m=0}^{\nu-1} \int_{-\infty}^{+\infty} \{H_{\nu}^{(1)}(k_2 r') H_{\nu}^{(1)}(k_2 r) [H_{\nu}^{(2)}(x)/H_{\nu}^{(1)}(x)] (1 + R_1)(1 + R_2) \cdot R_2^{\nu-1} [H_{\nu}^{(1)}(y)/H_{\nu}^{(2)}(y)]^{\nu} \exp [i\nu(\theta + 2\pi m)] d\nu, \quad (6c)$$

where (5e) and (5c) as well as (5d), (5f), and (5b) have been combined.

The denominator of (6c) contains the factor  $H_{\nu}^{(1)}(y) H_{\nu}^{(2)}(y)$  which increases exponentially when  $\nu > y$ . The principal contribution of those integrals therefore occurs in

the range  $(-y, y)$ . Substitution of the Debye asymptotic forms in this interval yields

$$I_{pm} \sim (4\pi)^{-1} \exp [i\pi(p - 1)/2] \int_{-A}^{+A} \frac{(1 + R_1)(1 + R_2)(-R_2)^{p-1}[1 + O(y^{-1})]}{\{[(k_2 r')^2 - \nu^2][(k_2 r')^2 - \nu^2]\}^{1/4}} d\nu, \tag{7a}$$

where

$$0 < y - A = O(y),$$

$$R_1 \sim -R_2 \sim \frac{(x^2 - \nu^2)^{1/2} - (y^2 - \nu^2)^{1/2}}{(x^2 - \nu^2)^{1/2} + (y^2 - \nu^2)^{1/2}}. \tag{7b}$$

The phase of the integrand is

$$\Theta = [(k_2 r')^2 - \nu^2]^{1/2} + [(k_2 r)^2 - \nu^2]^{1/2} - 2(x^2 - \nu^2)^{1/2} + 2p(y^2 - \nu^2)^{1/2} + \nu\{-\cos^{-1}(\nu/k_2 r') - \cos^{-1}(\nu/k_2 r) + 2\cos^{-1}(\nu/x) - 2p\cos^{-1}(\nu/y) + \theta + 2\pi m\}, \tag{7c}$$

where the inverse cosine functions are bounded by 0 and  $\pi$ . If  $\nu_\mu$  is a point of stationary phase, the condition  $\partial\Theta/\partial\nu |_{\nu_\mu} = 0$  leads to

$$\cos^{-1}(\nu_\mu/k_2 r') + \cos^{-1}(\nu_\mu/k_2 r) - 2\cos^{-1}(\nu_\mu/x) + 2p\cos^{-1}(\nu_\mu/y) = \theta + 2\pi m. \tag{8}$$

This equation does not have solutions for all values of  $m$  and  $p$ . For a fixed value of  $p$ , for example, the left side of (8) has a maximum in  $(-A, A)$  which always occurs at  $\nu_\mu = -A$ . As  $A$  approaches  $y$  this maximum value approaches  $2\pi p - U$ , where

$$U = \cos^{-1}(y/k_2 r') + \cos^{-1}(y/k_2 r) - 2\cos^{-1}N.$$

On the other hand, at  $\nu_\mu = A$  the value is minimum and approaches  $U$  as  $A$  approaches  $y$ . Since the right hand side of (8) must be within these limits, the possible values of  $m$  satisfy

$$2\pi p - (U + \theta) > 2\pi m > U - \theta.$$

But  $m$  is an integer, and  $\pi > U > 0, \pi \geq \theta \geq 0$  so that

$$p - 1 \geq m \geq 1.$$

It is clear that for  $m = 0$ , (8) has a solution only when  $\theta > U$ . The equation of the line separating regions 2 and 3 is  $\theta = U$  (see Fig. 1).

The stationary phase evaluation of (7a) yields

$$I_{pm} \sim \frac{(2/\pi)^{1/2}(1+R_{1\mu})(1+R_{2\mu})(-R_{2\mu})^{p-1} \exp\{i[\pi/4 + (p-1)\pi/2]\} \exp(i\Theta_\mu)[1+O(y^{-1})]}{\{[(k_2 r')^2 - \nu_\mu^2][(k_2 r)^2 - \nu_\mu^2]\}^{1/4} D^{1/2}}, \tag{9a}$$

$$D = 2p(y^2 - \nu_\mu^2)^{-1/2} - 2(x^2 - \nu_\mu^2)^{-1/2} + [(k_2 r')^2 - \nu_\mu^2]^{-1/2} + [(k_2 r)^2 - \nu_\mu^2]^{-1/2}, \tag{9b}$$

where the subscript  $\mu$  denotes evaluation at  $\nu_\mu$ , and in particular

$$\Theta_\mu = k_2\{[r'^2 - (\nu_\mu/k_2)^2]^{1/2} + [r^2 - (\nu_\mu/k_2)^2]^{1/2} - 2[a^2 - (\nu_\mu/k_2)^2]^{1/2}\} + 2pk_1[a^2 - (\nu_\mu/k_1)^2]^{1/2}. \tag{10}$$

The physical interpretation of these results as the rays of geometric optics is given in [1]. We note briefly that the function multiplying  $k_2$  in (10) is the distance the ray travels outside the cylinder, while the multiplicand of  $k_1$  corresponds to the  $p$  equal

paths the ray traverses inside. Thus the rays undergo  $p - 1$  internal reflections as is borne out by the factor  $R_{2\mu}^{p-1}$ , since the quantities  $R_{1\mu}$ ,  $R_{2\mu}$ ,  $(1 + R_{1\mu})$ , and  $(1 + R_{2\mu})$  are the Fresnel reflection and transmission coefficients. Furthermore when  $m < p/2$  the ray encircles the origin  $m$  times in a counterclockwise direction, while for  $m \geq p/2$ , the clockwise encirclements are given by  $p - m$ . The localization principle [5] as well as Snell's law are verified by the interpretation of  $v_\mu/k$  as the distance from the ray to the origin, where  $k = k_2$  for the external ray and  $k_1$  for the internal. If  $\alpha_i$  and  $\alpha_r$  are respectively the angles of incidence and refraction we have

$$\sin \alpha_i = v_\mu/k_2, \quad \sin \alpha_r = v_\mu/k_1,$$

so that

$$\sin \alpha_i / \sin \alpha_r = k_1/k_2 = N,$$

which is Snell's law. These quantities are illustrated in Fig. 2.

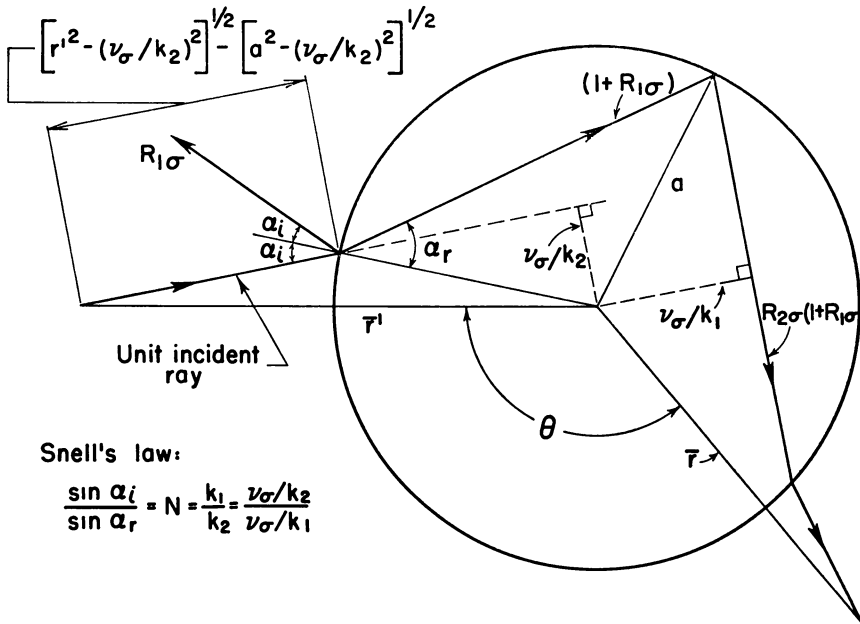


FIG. 2. A refracted ray,  $p = 2, m = 1$ .

The integrals in (6a) and (6b) do not have stationary points in region 1; they are evaluated as residue sums. Only the lower half plane solutions of  $C_1(\nu) = 0$  are used to locate the poles of  $R(\nu)$  since with  $m < 0$  the integrals (6a) require that the contour be closed below the axis. The pole locations  $\nu = -\nu_l$ , as computed in [6] are shown in Fig. 3. The integrals in (6b) are similarly evaluated at the poles of  $R(-\nu)$  in the upper half plane, i.e. at  $\nu = \nu_l$ . Thus (6a) is equal to

$$i \sum_{m=-\infty}^{-1} \sum_{\nu_l} \frac{H_\nu^{(1)}(k_2 r') H_\nu^{(1)}(k_2 r) \exp[-i\nu(\theta + 2\pi m)]}{[H_\nu^{(1)}(x)]^2 \partial_\nu C_1(\nu)|_{\nu=-\nu_l}},$$

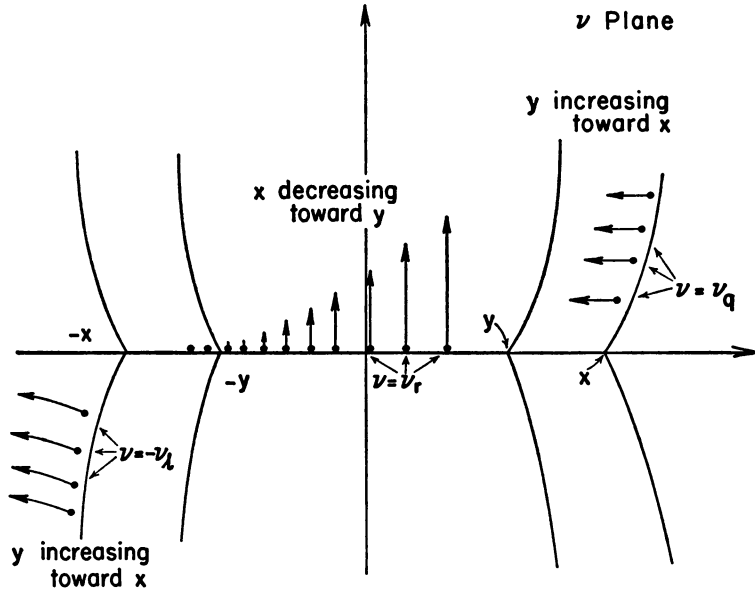


FIG. 3. Roots of  $xH_{\nu}^{(1)'}(x)/H_{\nu}^{(1)}(x) - yJ_{\nu}'(y)/J_{\nu}(y) = 0$ .

after employing the Wronskian relation. Under the conditions  $\nu_l - x = O(x^{1/3})$  and  $\nu_l - y = O(y)$ , the asymptotic form of this residue sum is

$$\sum_{m=-\infty}^{-1} \sum_{\nu_l} \frac{(2\pi)^{-1}(x/2)^{2/3} \exp \{i[\psi_1 - \nu(\theta + 2\pi m)]\} [1 + O(x^{-1})]}{\{[(k_2 r')^2 - \nu^2][(k_2 r)^2 - \nu^2]\}^{1/4} \{p(x, \nu) Ai[-q \exp(-i\pi/3)]\}^2 \partial_{\nu} C_1(\nu)|_{\nu=-\nu_l}}, \quad (11a)$$

where

$$\partial_{\nu} C_1|_{\nu=-\nu_l} = -(\nu_l^2 - y^2)/x + 4(\nu_l^2 - y^2)(\nu_l - x)/15x^2 + 2(\nu_l - x) + O(1), \quad (11b)$$

$$\psi_1 = k_2 \{ [r'^2 - (\nu/k_2)^2]^{1/2} + [r^2 - (\nu/k_2)^2]^{1/2} \} - \nu [\cos^{-1}(\nu/k_2 r') + \cos^{-1}(\nu/k_2 r)],$$

$p(x, \nu)$  and  $q$  are the Schöbe polynomials [4], and  $Ai(\tau)$  is the Airy function of the first kind. Similarly (6b) becomes

$$\sum_{m=0}^{+\infty} \sum_{\nu_l} \frac{(2\pi)^{-1}(x/2)^{2/3} \exp \{i[\psi_1 + \nu(\theta + 2\pi m)]\} [1 + O(x^{-1})]}{\{[(k_2 r')^2 - \nu^2][(k_2 r)^2 - \nu^2]\}^{1/4} \{p(x, \nu) Ai[-q \exp(-i\pi/3)]\}^2 \partial_{\nu} C_1(-\nu)|_{\nu=-\nu_l}}, \quad (12)$$

where the derivative is given by (11b).

The terms (11a) and (12) represent the well-known creeping waves [1], which radiate tangentially as they propagate around the cylinder. The exponential decay depends on the product of the angle and  $\text{Im}(\nu_l)$ . Thus the only important contributions are from the first encirclement, i.e.  $m = 0$  and  $m = -1$ . Physically, the waves have radiated away so much energy in their first encirclement that their next contribution is negligible. The localization principle can be applied to these waves also since  $\nu_l \approx x$  for the counter-clockwise waves which are associated with rays striking the cylinder tangentially in  $\theta > 0$ ; for the clockwise waves,  $-\nu_l \approx -x$ , and the tangential rays are incident in  $\theta < 0$ . The geometric model is illustrated in Fig. 4.

For  $\theta = \pi$ , the terms in (11a) and (12) are identical since the geometry is symmetric about  $\theta = 0, \pi$ . Further, the residue sum for  $m = 0$  does not converge when

$$\cos^{-1}(x/k_2r) + \cos^{-1}(x/k_2r') = \theta,$$

which defines the common boundary of regions 1 and 2. Here the observation point moves into the region of direct illumination, and the integral with  $m = 0$  gives optical rays.

**Region 2.** In region 2 it is convenient to rewrite the integral in (6b) with  $m = 0$  as,

$$(i/8) \int_{-\infty}^{+\infty} \{H_v^{(1)}(k_2r')H_v^{(2)}(k_2r) + H_v^{(1)}(k_2r')H_v^{(1)}(k_2r)[H_v^{(2)}(x)/H_v^{(1)}(x)]R_1(\nu)\} \exp(i\nu\theta) d\nu \quad (13a)$$

$$- (1/\pi^2) \int_{-\infty}^{+\infty} \frac{H_v^{(1)}(k_2r')H_v^{(1)}(k_2r) \exp(i\nu\theta) d\nu}{[H_v^{(1)}(x)]^2 H_v^{(2)}(y) J_{-\nu}(y) L(\nu) C_1(-\nu)}. \quad (13b)$$

The first of these integrals (13a) is evaluated by the stationary phase technique. We obtain in part

$$(i/4)(2/\pi)^{1/2} \frac{\exp[i(k_2|r-r'| - \pi/4)]}{(k_2|r-r'|)^{1/2}} \{1 + O[(k_2r)^{-1}]\},$$

which is just the first term in the asymptotic series for  $(i/4)H_0^{(1)}(k_2|r-r'|)$ , the free

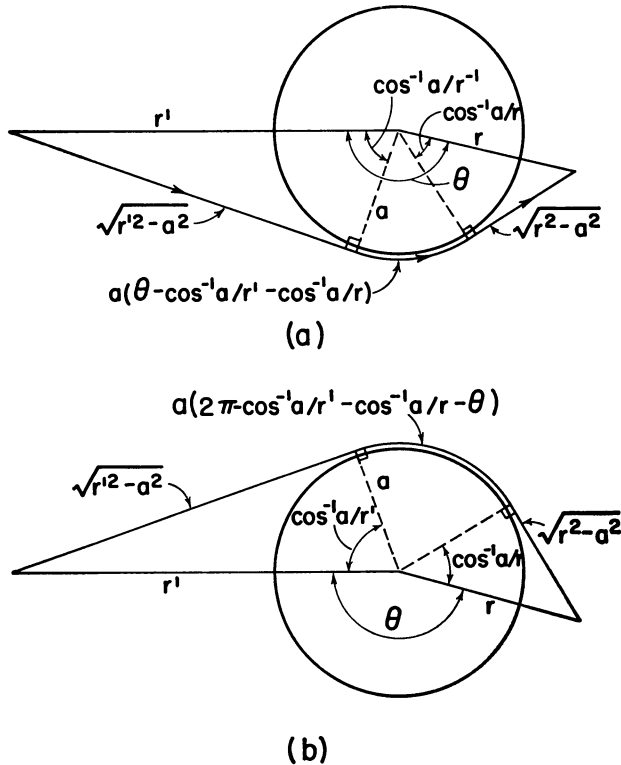


FIG. 4. Creeping waves.

space Green's function or equivalently the direct ray. In addition (13a) yields the singly reflected ray

$$\frac{R_{1\mu} \exp [i(\Theta_\mu + \pi/4)][1 + O(x^{-1})]}{2(2\pi)^{1/2} \{ [(k_2 r')^2 - \nu_\mu^2][(k_2 r)^2 - \nu_\mu^2] \}^{1/4} W^{1/2}},$$

where

$$\begin{aligned} \Theta_\mu &= k_2 \{ [r'^2 - (\nu_\mu/k_2)^2]^{1/2} + [r^2 - (\nu_\mu/k_2)^2]^{1/2} - 2[a^2 - (\nu_\mu/k_2)^2] \}, \\ W &= 2(x^2 - \nu_\mu^2)^{-1/2} - [(k_2 r')^2 - \nu_\mu^2]^{-1/2} - [(k_2 r)^2 - \nu_\mu^2]^{-1/2}, \\ R_{1\mu} &= [(x^2 - \nu_\mu^2)^{1/2} - (y^2 - \nu_\mu^2)^{1/2}] / [(x^2 - \nu_\mu^2)^{1/2} + (y^2 - \nu_\mu^2)^{1/2}], \\ (y^2 - \nu_\mu^2)^{1/2} &= -i(\nu_\mu^2 - y^2)^{1/2}, \end{aligned}$$

and  $\nu_\mu$  is the solution of

$$\cos^{-1}(\nu_\mu/k_2 r') + \cos^{-1}(\nu_\mu/k_2 r) - 2 \cos^{-1}(\nu_\mu/x) = \theta.$$

Here we have neglected the phase contributed by  $R_1(\nu)$  for  $\nu > y$  since it is of a lower order than that given by the Hankel functions.

The integral (13b) is evaluated as a residue sum at the poles of the integrand in the upper half plane. These are the solutions of  $L(\nu) = 0$ ,

$$xH_\nu^{(1)'}(x)/H_\nu^{(1)}(x) - yH_\nu^{(2)'}(y)/H_\nu^{(2)}(y) = 0, \tag{14a}$$

as well as the solutions of  $C_1(-\nu) = 0$ ,

$$xH_\nu^{(1)'}(x)/H_\nu^{(1)}(x) - yJ'_-(y)/J_-(y) = 0. \tag{14b}$$

The solutions of (14b) in the upper half plane are  $\nu_i$ , while those of (14a) are  $\nu_i$  and  $\nu_s$  (see Fig. 5). Thus it appears that double poles exist at  $\nu_i$ ; however, an examination of equations (14a) and (14b) shows that these solutions are not exactly coincident and in fact depend on  $2J_-(y) \sim H_{-\nu}^{(2)}(y)$  in this part of the  $\nu$ -plane. By writing  $\nu'_i$  for the roots of (14a) and  $\nu''_i$  for those of (14b) we show in Appendix B that the total residue at  $\nu_i$  is negligible.

Thus (13b) is equal to

$$i \sum_{\nu_i} \frac{H_\nu^{(1)}(k_2 r') H_\nu^{(1)}(k_2 r) \exp(i\nu\theta)}{[H_\nu^{(1)}(x)]^2 [\partial L / \partial \nu]_{\nu_i}},$$

which becomes after substitution of the asymptotic forms

$$i \sum_{\nu_i} \left\{ \frac{(x^2 - \nu^2)^2}{[(k_2 r')^2 - \nu^2][(k_2 r)^2 - \nu^2]} \right\}^{1/4} \frac{\exp [i(\psi_2 + \nu\theta)][1 + O(x^{-1})]}{[\partial L / \partial \nu]_{\nu_i}}, \tag{15a}$$

where

$$\begin{aligned} \psi_2 &= k_2 \{ [r'^2 - (\nu/k_2)^2]^{1/2} + [r^2 - (\nu/k_2)^2]^{1/2} - 2[a^2 - (\nu/k_2)^2]^{1/2} \} \\ &\quad - \nu [\cos^{-1}(\nu/k_2 r') + \cos^{-1}(\nu/k_2 r) - 2 \cos^{-1}(\nu/x)], \end{aligned} \tag{15b}$$

$$\partial L / \partial \nu|_{\nu_i} \sim -(x^2 - \nu_i^2)/y + 4(x^2 - \nu_i^2)(\nu_s - y)/15y^2 + 2(\nu_s - y) + O(1) = O(x). \tag{15c}$$

It is possible to interpret formula (15a) in terms of ray optics, but not as clearly as in the creeping wave situation. Since  $\nu_s \approx -y + i \text{Im}(\nu_s)$  where  $\text{Im}(\nu_s) > 0$ , the localization principle relates these terms to the rays which strike the cylinder at the angle



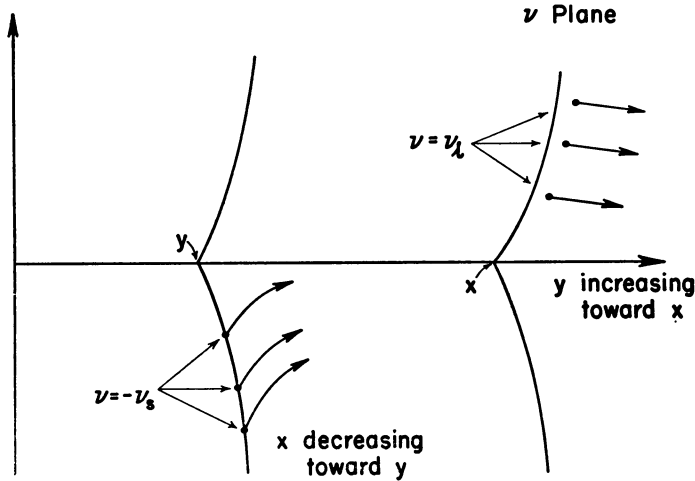


FIG. 5. Roots of  $xH_1^{(1)'}(x)/H_1^{(1)}(x) - yH_2^{(2)'}(y)/H_2^{(2)}(y) = 0$  in the right half plane.

of total reflection above the line  $\theta = 0$ . The first phase term in (15b) is the product of  $k_2$  and a distance consistent with the above interpretation (see Fig. 6). The second phase term

$$-i\nu_s[\cos^{-1}(\nu_s/k_2r') + \cos^{-1}(\nu_s/k_2r) - 2\cos^{-1}(\nu_s/x) - \theta]$$

is approximately equal to

$$i\nu_s[\theta + \cos^{-1}(Na/r') + \cos^{-1}(Na/r) - 2\cos^{-1}N],$$

which is  $i\nu_s$  multiplying the angle  $\Omega$  shown in Fig. 6. Thus this part of the phase represents a wave traveling counterclockwise around the cylinder with propagation constant  $\nu_s$ .

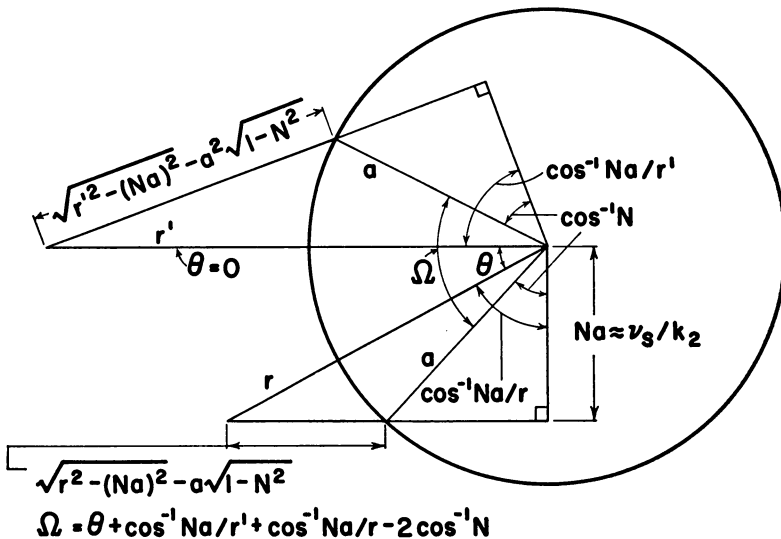


FIG. 6. Physical interpretation of residues, equation (15a).

Since  $\text{Im}(\nu_s) > 0$ , the exponential in (15a) has a negative real part and the wave decays in proportion to the angle; however, the  $\text{Re}(\nu_s)$  is negative and so the physical interpretation is not completely satisfactory.

**Region 3.** The results derived above for (13a) and (13b) are applicable to observation points in region 3. The integrals (5e), however, as was mentioned in connection with Eq. (8), have no stationary phase points in region 3. After summation (5e) is equal to

$$-(i/\pi^2) \int_{-\infty}^{+\infty} \frac{H_\nu^{(1)}(k_2 r') H_\nu^{(1)}(k_2 r) \exp(i\nu\theta) d\nu}{[H_\nu^{(1)}(x)]^2 H_\nu^{(2)}(y) J_\nu(y) L(\nu) C_1(\nu)}, \tag{16}$$

which is evaluated by residues.

For  $\theta > 0$ , the contour may only be closed by an infinite semicircle in the upper half plane. The four residue series obtained from the poles  $\nu_l, \nu_s, \nu_a$ , and  $\nu_r$  (see Figs. 3 and 5) converge so slowly that one could as well employ the series solution (2a). It is possible, however, to approximate (16) by deforming the path of integration as shown in Fig. 7.

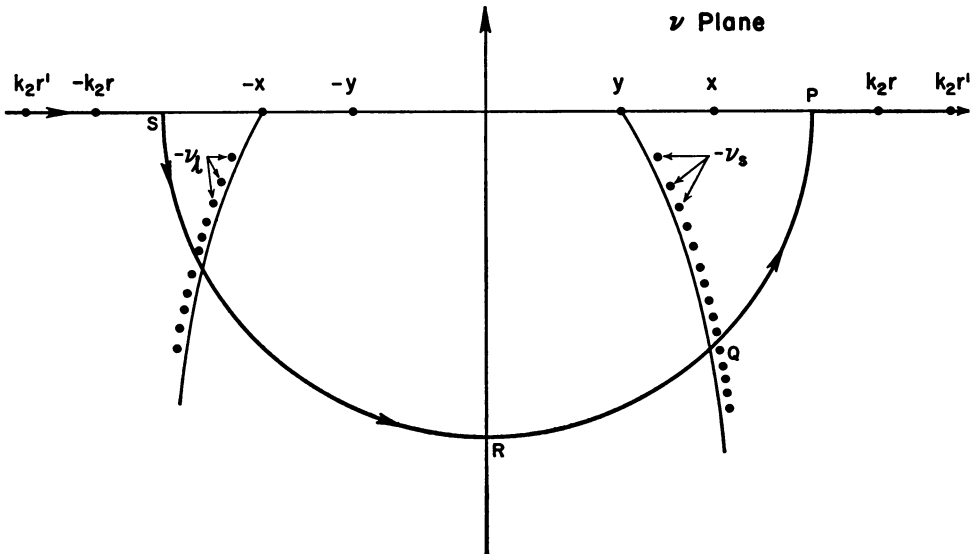


FIG. 7. Deformed path of integration.

The integral over the new path is neglected compared to the residues at the captured poles,  $-\nu_s$ , (see Appendix C). We note that the residues at the captured poles,  $-\nu_l$ , are negligible as shown in Appendix B. Thus (16) is approximately equal to

$$i \sum_{\nu_s} \left\{ \frac{(x^2 - \nu^2)^2}{[(k_2 r')^2 - \nu^2][(k_2 r)^2 - \nu^2]} \right\}^{1/4} \frac{\exp[i(\psi_2 - \nu\theta)][1 + O(x^{-1})]}{[\partial L / \partial \nu]_{\nu_s}}, \tag{17}$$

where the summation includes only captured poles and  $\psi_2$  and the derivative are given by (15b) and (15c) respectively. In region 3 the inequality

$$\cos^{-1}(Na/r') + \cos^{-1}(Na/r) - 2 \cos^{-1}(N) > \theta \tag{18}$$

is satisfied and successive terms in (17) have decreasing magnitudes.

The form of (17) is the same as (15a) with the sign of  $\theta$  reversed; indeed for  $\theta = 0$  the integrals (16) and (13b) are identical. The physical interpretation of the residues at  $\nu_s$  and  $-\nu_s$  is similar except that the former are associated with rays incident in  $\theta > 0$ .

**Plane waves and back-scattering.** To specialize the above results to the case of an incident plane wave of unit amplitude, one simply applies the operator

$$\lim_{r' \rightarrow \infty} \{-4i(\pi k_2 r'/2)^{1/2} \exp [i(\pi/4 - k_2 r')]\}$$

to the previous results. We choose here to consider the case of back-scattering since the other case of chief interest, the scattering cross section, cannot be completely treated by the methods developed above.

The normalized back-scattering cross section is defined by

$$\sigma_B = |\lim_{r \rightarrow \infty} (2r/a)^{1/2} E_s(\theta = 0)|^2 = |E_R|^2,$$

where  $E_s$  is the scattered field, and

$$E_R = [(1 - N)/(1 + N)] \exp(-2ix) + \sum_{p=2}^{\infty} \sum_{m=1}^{p-1} (1 + R_{1\mu})(1 + R_{2\mu})(-R_{2\mu})^{p-1} (\cos \alpha_i)^{1/2} \cdot [(p \cos \alpha_i / N \cos \alpha_r) - 1]^{-1/2} \exp[-2ix(1 - pN \cos \alpha_r / \cos \alpha_i) + i(p - 1)\pi/2] \quad (19a)$$

$$+ \sum_{m=1}^{\infty} \sum_{\nu_1} \frac{4(x/2)^{2/3} \exp [i\nu_1(2m - 1)\pi + i\pi/4]}{(\nu_1^2 - y^2) \{p(x, \nu_1) Ai[-q(x, \nu_1) \exp(-i\pi/3)]\}^2} \quad (19b)$$

$$- \sum_{\nu_s} 8(\pi/2)^{1/2} y(x^2 - \nu_s^2)^{-1/2} \exp \{-2i(x^2 - \nu_s^2)^{1/2} - i\nu_s[\pi - 2 \cos^{-1}(\nu_s/x)] - i\pi/4\}, \quad (19c)$$

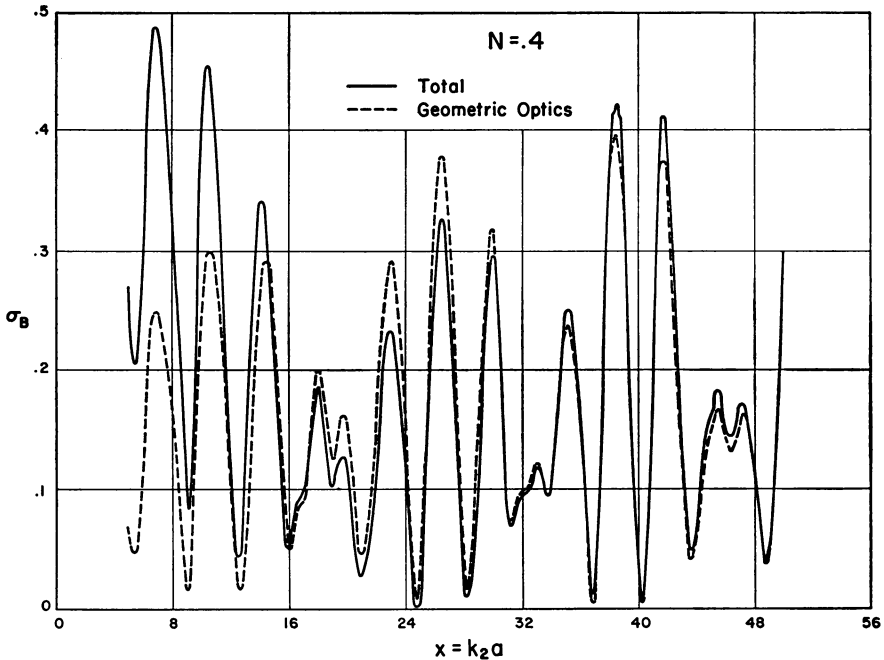


FIG. 8. Normalized back-scattering cross section vs.  $x$ .

with  $\cos \alpha_i = (1 - \nu_i^2/x^2)$  and  $\cos \alpha_r = (1 - \nu_i^2/y^2)$ . The calculation of  $\sigma_B$  was programmed for the IBM 7070 of the Brown University Computing Center. The geometric optics terms in (19a) required the iterative solution of  $\sin \alpha_i = N \sin \alpha_r$  and  $\alpha_r = [\alpha_i - \pi(p/2 - m)]/p$ . The creeping wave terms represented by (19b) were found to be negligible and only (19c) contributed to the diffraction effect. Figure 8 is a plot of  $\sigma_B$  vs.  $k_2a$  for  $N = .4$ .

The results developed here do not apply to observation points near  $\theta = \pi$  and the boundaries separating regions 1, 2 and 3 since these lines are caustics. Thus the forward scatter with an incident plane wave has not been completely determined and the scattering cross section cannot be calculated.

APPENDIX A

The power series (4a)

$$R(\nu) = R_1(\nu) + (1 + R_1)(1 + R_2) \sum_{p=1}^{+\infty} R_2^{p-1} [H_\nu^{(1)}(y)/H_\nu^{(2)}(y)]^p$$

converges by the ratio test when

$$|R_2 H_\nu^{(2)}(y)/H_\nu^{(1)}(y)| < 1.$$

On the real  $\nu$  axis this condition becomes  $|R_2| < 1$  or  $R_2 R_2^* < 1$ . We write

$$R_2 = -(D - NE)/(D - NE^*),$$

so that

$$R_2 R_2^* = \frac{|D|^2 + N^2 |E|^2 - N(ED^* + DE^*)}{|D|^2 + N^2 |E|^2 - N(E^*D^* + DE)}. \tag{A-1}$$

We have however,

$$ED^* + DE^* - (E^*D^* + DE) = -(D - D^*)(E - E^*), \tag{A-2}$$

where

$$D - D^* = H_\nu^{(1)'}(x)/H_\nu^{(1)}(x) - H_\nu^{(2)'}(x)/H_\nu^{(2)}(x) = (4i/\pi x) |H_\nu^{(1)}(x)|^{-2}$$

and

$$E - E^* = (4i/\pi y) |H_\nu^{(1)}(y)|^{-2},$$

so that (A-2) is positive definite. This implies that (A-1) is less than unity and the series converges.

APPENDIX B

At the solutions of (14a),  $\nu_i'$ , the residue calculation gives for the denominator of (13b)

$$H_{-\nu}^{(2)}(y)J_{-\nu}(y)C_1(-\nu)[\partial L/\partial \nu]_{\nu_i'} = -(2i/\pi)[\partial L/\partial \nu]_{\nu_i'},$$

where the Wronskian relation has been employed. Similarly at the solution of (14b),  $\nu_i''$ , we have

$$H_{-\nu}^{(2)}(y)J_{-\nu}(y)L(\nu)[\partial C_1(-\nu)/\partial \nu]_{\nu_i''} = (2i/\pi)[\partial C_1(-\nu)/\partial \nu]_{\nu_i''}.$$

Adding the two residues and setting  $\nu'_i = \nu''_i = \nu_i$ , the result is

$$\begin{aligned} & \{(\pi y/2i)[\partial C_2(-\nu)/\partial \nu]\} / \{(\partial L/\partial \nu)[\partial C_1(-\nu)/\partial \nu]\} \\ & \sim - \frac{\partial \{ [H_{\nu_i}^{(2)}(y)]^{-2} \exp(2\pi i \nu) \} / \partial \nu}{(\partial L/\partial \nu)^2} \sim \frac{2x^2 \cosh^{-1}(\nu_i/y) \exp(2\pi i \nu_i)}{(\nu_i^2 - y^2) [H_{\nu_i}^{(2)}(y)]^2}, \end{aligned}$$

which is very small since  $\text{Im}(\nu_i) > 0$  and  $H_{\nu_i}^{(2)}(y)$  increases as an exponential function of  $\nu_i$ .

The residues of (16) at  $-\nu_i$  yield the same result, as substitution of  $-\nu$  for  $\nu$  will show.

APPENDIX C

On those parts of the path shown in Fig. 7, which coincide with the real axis, the integrand of (16)

$$H_{\nu}^{(1)}(k_2 r') H_{\nu}^{(1)}(k_2 r) \exp(i\nu\theta) / [H_{\nu}^{(1)}(x)]^2 H_{\nu}^{(2)}(y) J_{\nu}(y) L(\nu) C_1(\nu) \tag{C-1}$$

has an exponential variation given by

$$H_{\nu}^{(1)}(k_2 r') H_{\nu}^{(1)}(k_2 r) \exp(i\nu\theta) / [H_{\nu}^{(1)}(x)]^2. \tag{C-2}$$

When  $|\nu| > x$  and  $|\nu| - x = O(x)$ , (C-2) is very small and decreases rapidly with increasing  $|\nu|$ .

The exponential variation of (C-1) on the circular part of the path changes from (C-2) on the arc  $PQ$  to

$$H_{\nu}^{(1)}(k_2 r') H_{\nu}^{(1)}(k_2 r) \exp(i\nu\theta) / [H_{\nu}^{(1)}(x)]^2 [H_{\nu}^{(2)}(y)]^2 \tag{C-3}$$

on the arc  $QRS$  (see Fig. 7). Since (C-2) is symmetric about the imaginary axis and  $[H_{\nu}^{(2)}(y)]^{-2}$  is very small in the third quadrant, the maximum value of (C-1) occurs on the arc  $PQR$ . Along  $PQR$ , (C-2) increases from

$$\exp[2(\nu^2 - x^2)^{1/2} - 2\nu \cosh^{-1}(\nu/x)]$$

at  $P$ , to  $\exp(i\nu\theta)$  at  $R$ . However, (C-3) must be employed at points between  $Q$  and  $R$ , and the additional quantity  $[H_{\nu}^{(2)}(y)]^{-2}$  varies exponentially from unity at  $Q$  to  $\exp(-i\nu\pi)$  at  $R$ . Thus the integrand (C-1) attains its maximum value in the vicinity of  $Q$ .

At  $Q$  the exponential variation of (C-1) is

$$\begin{aligned} & \exp \{ i[(k_2 r')^2 - \nu^2]^{1/2} + [(k_2 r)^2 - \nu^2]^{1/2} - 2(x^2 - \nu^2)^{1/2} \\ & - i\nu[\cos^{-1}(\nu/k_2 r') + \cos^{-1}(\nu/k_2 r) - 2 \cos^{-1}(\nu/x) + \theta] \}, \end{aligned} \tag{C-4}$$

and the equation of the curve passing through  $Q$  is

$$\text{Im} [(y^2 - \nu^2)^{1/2} - \nu \cos^{-1}(\nu/y)] = 0. \tag{C-5}$$

Since a general examination of (C-4) subject to (C-5) is quite complicated, a numerical example will be considered. Let  $k_2 r', k_2 r = 3.5x$ ,  $N = y/x = .5$ , and  $\nu = 1.4x$ . An approximate solution of (C-5) yields  $\nu = 1.4x \exp(-i\pi/4)$  and (C-4) is approximately equal to  $\exp x(-1.27 + \theta)$ . From (18), which defines region 3, we obtain  $\theta < .76$  radians and the integral over the semicircle is negligible compared to the residues.

## REFERENCES

1. P. Beckmann and W. Franz, *Z. Naturf.* **12a**, 257 (1957)
2. P. Beckmann and W. Franz, *IRE AP-4*, **3** (1956)
3. T. T. Wu, *Phys. Rev.* **104**, 1201 (1956)
4. W. Streifer and R. D. Kodis, *Quart. Appl. Math.*, **21**, 285-297 (1964)
5. H. C. van de Hulst, *Light Scattering by Small Particles*, (John Wiley, 1957)
6. W. Streifer and R. D. Kodis, *Brown University Scientific Report AF 4561/18*, 1962